JOURNAL OF GEOPHYSICAL RESEARCH, VOL. 94, NO. C8, PAGES 10,755–10,772, AUGUST 15, 1989

Wintertime Air-Sea Interaction Processes Across the Gulf Stream

JOHN M. BANE, JR.,[1] AND KENRIC E. OSGOOD[2]

Marine Sciences Program, University of North Carolina, Chapel Hill

Aircraft, buoy and satellite measurements have been used to study the wintertime air-sea interaction processes across the Gulf Stream during January 25–30, 1986. The turbulent flux regime in the marine atmospheric boundary layer exhibited considerable spatial and temporal variability during this 6-day period, which was related to both the evolution of the synoptic scale atmospheric conditions and the sea surface temperature (SST) field. During the pre-storm conditions prior to January 25, the spatial structure of the SST field played an important role in generating a shallow atmospheric frontal zone along the Gulf Stream front by causing differential heating of the marine atmospheric boundary layer over the stream versus over the cooler shelf waters. As this front moved shoreward on January 25, the warm, moist, maritime air flowing northwestward behind the front induced moderate ocean-to-atmosphere heat fluxes (~300 W m^{-2} total heat flux measured over the core of the Gulf Stream). The subsequent outbreak of eastward flowing cold, dry, continental air over the ocean on January 27 and 28 generated high total heat fluxes (~1060 W m^{-2} over the core of the Stream), as did a second, somewhat weaker outbreak which followed on January 30 (~680 W m^{-2} over the core of the Stream). During each of these outbreaks, with air flowing from land out over the continental shelf, Gulf Stream and Sargasso Sea waters, the SST field again affected the spatial structure of the flux fields. The near-surface fluxes of both sensible and latent heat were found to be relatively low over the cool continental shelf waters, while higher fluxes were seen over the Gulf Stream and Sargasso Sea. Similar spatial structure was seen in the near-surface momentum flux values, but relative changes were typically smaller from one location to another on a particular day. The most noticeable responses of the Gulf Stream to these surface fluxes were the deepening of its mixed layer and a loss of upper layer heat; however, no direct current observations were made in the stream, so velocity changes may not be assessed. An average mixed layer deepening of about 35 m was observed in the stream, and the upper layer heat loss was estimated to be 3.2 x 10^{13} J m^{-1} alongstream, an amount sufficient to decrease the average mixed layer temperature by 0.62°C. No path changes in the stream could be attributed to the atmospheric forcing of this period, since there was a large offshore movement of the stream in the region of the Charleston bump at this time due to other processes. Any path changes that may have been associated with the atmospheric forcing would have been masked by that offshore movement.

INTRODUCTION

In this paper we present aircraft, buoy and satellite observations that describe wintertime air-sea interaction processes across the Gulf Stream off the coast of the southeastern United States. We also show the Gulf Stream's upper layer thermal response to these interactions. The data were collected between January 25 and 30, 1986, as part of the Genesis of Atlantic Lows Experiment (GALE). During this time an atmospheric cyclone that had developed earlier over the northwestern United States, swept eastward toward New England and intensified. Weather within the study region off the coast of the southeastern United States progressed from "pre-storm" conditions to a strong cold air outbreak, followed by a weaker cold air outbreak. This case provided some of the strongest atmospheric forcing of the Gulf Stream during GALE, and it gives a view into the complex air-sea interactions typical of this area.

In the next section of this paper we provide a scientific background, and in the third section we discuss the methods of observation used during our study. A description of the meteorological events during the January 25–30 period then follows. In this description we give an overview of the storm system and its movement using GOES satellite imagery and near-surface measurements from an offshore meteorological buoy. We then focus on the study region and present detailed aircraft measurements of (1) the structure of the marine atmospheric boundary layer (MABL) over the continental shelf and Gulf Stream, (2) the variation with altitude of vertical, turbulent fluxes of momentum, sensible heat and latent heat within the MABL, and (3) the upper ocean thermal structure. Data from flights on January 25, 28, and 30 are given. Finally, we discuss the observed changes in the Gulf Stream's thermal structure during this period and consider the significance of such changes in light of the measured air-sea exchanges.

BACKGROUND

Extratropical winter cyclones that travel over the northwestern Atlantic Ocean provide some of the strongest meteorological forcing of that ocean region. Winds produced by these storms are strong, sometimes of hurricane strength, and can change in direction and magnitude rapidly as the storm progresses [*Sanders and Gyakum*, 1980; *Gyakum*, 1983*a*, *b*; *Sanders*, 1984, 1986*a*, *b*]. A maximum in the frequency of occurrence of winter cyclones off the U. S. east coast is located along a wide band centered on Cape Hatteras [*Colucci*, 1976]. Within this band many of the cyclones develop "explosively," exhibiting central pressure drops of more than 1 mbar h^{-1} for 24 hours or more [*Sanders and Gyakum*, 1980]. The studies of *Hayden* [1981], *Zishka and Smith* [1980],

[1]Also at Departments of Geology and Physics, University of North Carolina.

[2]Now at School of Oceanography, University of Washington, Seattle.

Paper number 89JC00373.
0148-0227/89/89JC-00373$05.00

and *Whittaker and Horn* [1981] suggest that an average of from 1.5 to 3 atmospheric cyclones pass through this area during a typical January, and possibly more during March. The GALE studies were situated here because of the high frequency of cyclone occurrence and strong cyclogenesis.

Fluctuations in atmospheric temperature, humidity and wind stress over the continental shelf and Gulf Stream in the GALE study area due to wintertime cyclones have periods of about 3–10 days. At a typical location in the GALE oceanographic study area, the cyclonic winds around a travelling storm's low pressure center are usually first noticeable as a southeasterly to southwesterly flow of warm, moist, maritime air (the storm's warm sector). This changes to a westerly to northerly flow of cold, dry, continental air following the passage of the storm's cold front (the cold air outbreak). As this cold, dry air flows out over the warm waters of the Gulf Stream and Sargasso Sea it induces very high fluxes of sensible and latent heat from the ocean to the atmosphere. According to *Budyko* [1974], these heat fluxes achieve their highest monthly averaged values in the world ocean over the Gulf Stream in winter (~430 W m^{-2} sensible plus latent heat flux). *Gorshkov* [1978], using 70 years of ship observations, indicates that the maximum yearly averaged latent heat flux (~240 W m^{-2}) occurs northeast of Cape Hatteras over the stream.

Prior to GALE a small number of cold air outbreaks had been studied in the vicinity of the Gulf Stream, over the Gulf of Mexico and over the Kuroshio Current. The recent work by *SethuRaman et al.* [1986] during a 5-day cruise off North Carolina in November 1983 sketched some of the instantaneous aspects of a mild cold air outbreak over the Gulf Stream. Ahead of a cold front passage through their study area, a southwesterly flow of tropical maritime air was observed, and the MABL thickness was about 500 m. The cold front then passed, and a cold air outbreak followed. The outbreak was characterized by a northwesterly flow of cold, dry, continental air, and the MABL thickness was observed to be about 1500 m in the presence of strong convective conditions. The MABL was also better defined during the outbreak with a strong thermal inversion at its upper boundary. Turbulent surface fluxes of sensible and latent heat were estimated with the bulk aerodynamic method. Sensible heat flux was almost negligible during the pre-frontal and frontal passage stages, whereas it was about 150 W m^{-2} during the cold air outbreak. The latent heat flux increased from about 100 W m^{-2} during prefrontal conditions to over 300 W m^{-2} during the outbreak. Air-sea temperature differences were about 10°C during this outbreak.

Over the northwest Florida Shelf in the Gulf of Mexico, *Huh et al.* [1984] reported that latent, sensible, and radiative heat losses accounted for 51, 16, and 33% of a total 52.9 x 10^6 J m^{-2} lost during a mild cold air outbreak. These losses changed to 58, 25, and 17% of a total 184.5 x 10^6 J m^{-2} lost during a severe outbreak. *Henry and Thompson* [1976] used radiosonde data from near New Orleans and Merida, Yucatan, Mexico, to deduce the heat fluxes along an air parcel trajectory over the Gulf of Mexico. Their budget calculation during cold northerly flow indicated a total average heat flux of 2400 W m^{-2} in the first 110 km of travel over the warm water. In their case the air over the coastline was near -4°C, and the water was about 20°C. *Chou and Atlas* [1982] have suggested that these fluxes are too large on the basis of a technique for determining mean air column heating from surface fluxes. Their method, developed from *Stage and Businger's* [1981*a*, *b*] boundary layer model for cold air outbreaks over warm water, gives estimates of 400 and 660 W m^{-2} for the average sensible and latent heat fluxes, respectively, over the same portion of the trajectory.

The Air Mass Transformation Experiment (AMTEX) studied the air-sea interaction processes during a cold air outbreak over the western North Pacific Ocean. AMTEX was conducted south of Japan during February 1974 and February 1975 in a location where cold continental air originating from the Asian land mass is modified through interactions with the warm waters of the Kuroshio. *Kondo* [1976] described the evolving meteorological patterns within the AMTEX area during the cold air outbreak of February 11–26, 1974. As the cold air penetrated southward and eastward, the values of the surface heat and momentum fluxes increased significantly. On February 26 the maximum wind stress was about 0.5 N m^{-2}, and the sensible and latent heat fluxes were in excess of 300 W m^{-2} and 800 W m^{-2}, respectively. The largest heat and momentum fluxes observed during the period first occurred near the coast and then progressed seaward with the leading edge of the cold air. The maximum values of the heat and momentum fluxes occurred over the Kuroshio as the cold, dry air interacted with the warm waters of the current.

The response of the Gulf Stream to strong atmospheric forcing is not well known. Several studies have suggested that the stream's position, circulation, and frontal structure are affected by air-sea interaction processes. The recent numerical simulations by *Adamec and Elsberry* [1985*a*, *b*] provide a model basis for describing the response of the Gulf Stream to atmospheric cooling and wind stress. Their model stream's response to horizontal cooling gradients is insufficient to significantly displace the stream seaward, as has been suggested by *Nof* [1983]. In contrast, a moderate increase in alongstream wind stress may efficiently displace the model current laterally. This wind-stress-induced effect is consistent with the observations of *Horton* [1984], who found the main response of the stream to forcing by hurricane Dennis in the region downstream from Cape Hatteras to be a surface layer shift due to Ekman advection. In a later study, however, *Horton and Horsley* [1988] reported that Ekman advection in the stream was not observed to be very important during a winter cyclone in that region.

Secondary, cross-stream currents with magnitudes from 0.3 cm s^{-1} [*Adamec and Elsberry*, 1985*b*] to 3 cm s^{-1} [*Nof*, 1983; *Adamec and Elsberry*, 1985*b*] have been observed in model simulations due to combined winds and cooling. The effects of strong surface cooling alone appear to steepen the Gulf Stream's temperature front and sharpen its temperature gradients [*Worthington*, 1976; *Adamec and Elsberry*, 1985*b*], while cooling, combined with alongstream wind stress provides competing mechanisms, which may actually result in frontal weakening [*Adamec and Elsberry*, 1985*b*]. *Worthington* [1977] has postulated that an abnormally cold winter season will accelerate the Gulf Stream through enhanced differential cross-stream cooling.

METHODS

During our GALE air-sea interaction study, simultaneous measurements of upper ocean thermal structure and MABL structure were made on vertical sections across the continental shelf and Gulf Stream. These measurements were conducted from the NOAA P-3 and the NCAR Electra research aircraft using on-board instrumentation for MABL variables and sea surface temperature (SST) and using air-deployed expendable bathythermographs (AXBTs) for subsurface ocean temperature (P-3 only). P-3 flights were made on January 25 and 30, and an Electra flight was made on January 28.

We present in this paper two types of aircraft-measured atmospheric data. Synoptic scale wind, temperature, and humidity

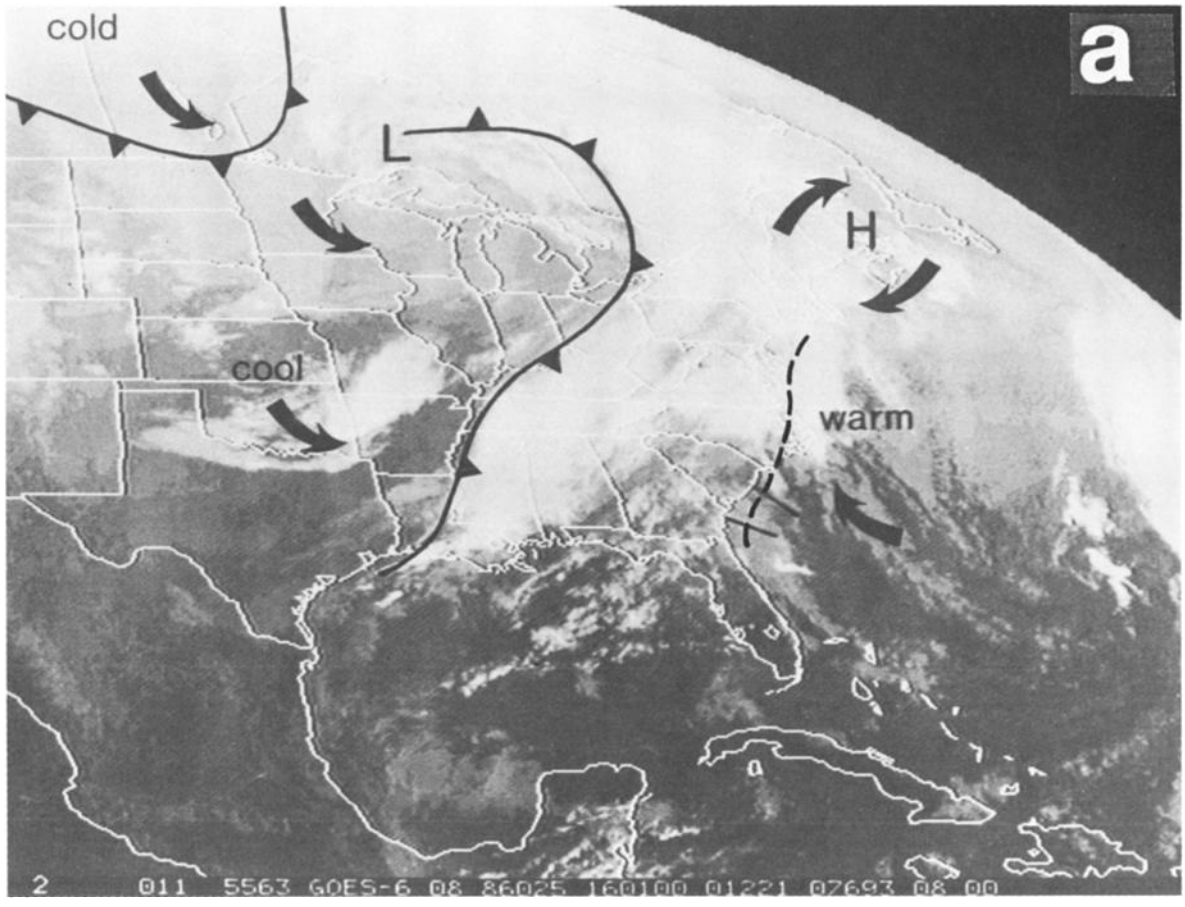

Fig. 1. GOES satellite images showing the meteorological conditions during the study. Low (L) and high (H) pressure centers, surface cold fronts, and general surface level winds taken from surface charts are depicted on each image. The flight tracks flown within the study area on each day are shown by the short, solid lines extending seaward from the coastline of the southeastern United States. Pre-storm conditions prevailed in the study area on January 25 (Figure 1*a*) with a southeasterly flow of warm, maritime air. Moving landward ahead of this air was a coastal front, which was just off and along the coast of the Carolinas at the time of this image (dashed line). The cold air behind the strong cold front (northwest of the low (L) that was positioned north of the Great Lakes at this time) is the air mass that moved down across the eastern United States and out over the ocean during the next few days. That cold air may be seen sweeping out across the entire eastern seaboard on January 28 (Figure 1*b*). Near-surface winds within the study area during this cold air outbreak were westerly at 10 m s^{-1} or more. On January 30 (Figure 1*c*) the strong cold front had moved farther east, and a second, somewhat weaker cold front had just moved through the study area as a result of another low pressure center (L_2) that had formed during the previous 2 days. Winds in the study area were northerly at about 8–9 m s^{-1} during this second cold air outbreak. (Images prepared by C. Velden.)

data were collected with each aircraft's on-board "slow rate" sensors [*Merceret and Davis*, 1981; *Miller and Friesen*, 1985] in order to determine MABL structure. Atmospheric turbulence quantities (velocity, temperature, and humidity) were measured with the "fast rate" turbulence system aboard each aircraft [*Greenhut and Gilmer*, 1985; *Miller and Friesen*, 1985]. Vertical "stack" patterns were flown to gather turbulence data at several levels within the MABL. A stack is composed of a number of straight and level flight legs, each one flown for several minutes at a prescribed altitude to gather time series of the appropriate variables. By "stacking" several legs over one another, a vertical profile may be determined. The measured time series were subsequently used in computing vertical turbulent fluxes at the altitude of each stack leg using the correlation method.

An intercomparison between the P-3 and the Electra was performed in the study region during GALE, and a synopsis of the results from that effort is presented in the appendix (see also *Osgood et al.* [1987]). No differences were found between the two aircraft measurement systems that would present significant problems with the analysis presented herein.

Ocean subsurface temperatures were measured with Sippican 305-m AXBTs deployed from the P-3 on the January 25 and 30 flights. Sections were flown in the cross-stream direction, and lateral AXBT station spacing was about 12.5 km. Calibration information on the manufacturer's lot of AXBTs used in GALE was gathered during a flight that deployed several AXBTs next to the R/V *Cape Hatteras*, which was collecting conductivity-temperature-depth (CTD) profiles at the time. On the January 25 and 30 P-3 flights and on the January 28 Electra flight, SST was measured with a Barnes PRT-5 infrared radiometer. Data collected on all of the P-3 flights conducted during our GALE Gulf Stream studies, plus the AXBT calibration procedure and results are documented by *Osgood and Bane* [1987].

THE METEOROLOGICAL SETTING

The storm system on which we focus was the main topic of study during GALE intensive observation period 2 (IOP 2). The conditions during the period January 25–30, 1986, are described in this section with the aid of GOES satellite images (Figure 1) and data from GALE meteorological buoy 5 (Figure 2). The

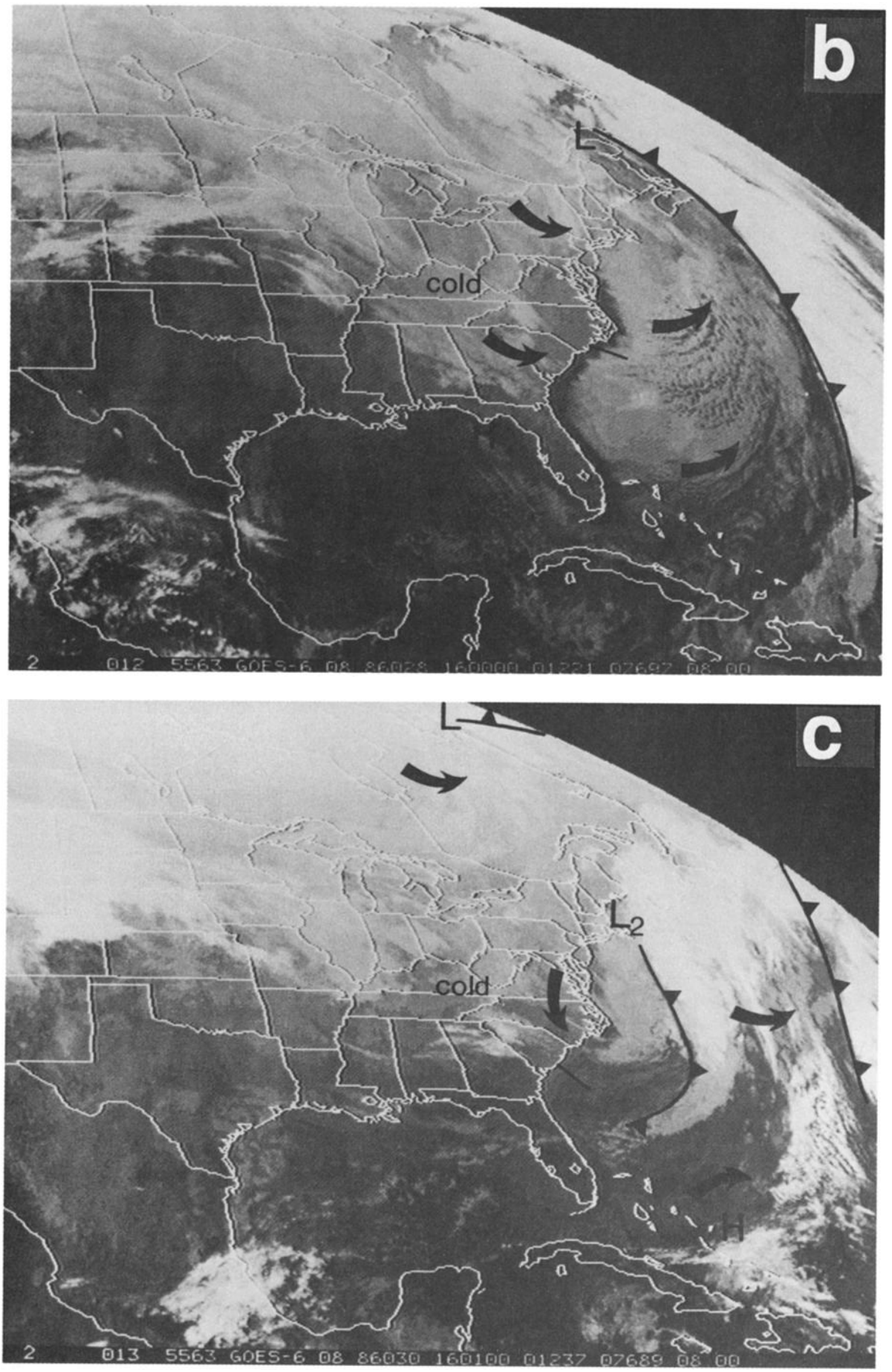

Fig. 1. (continued)

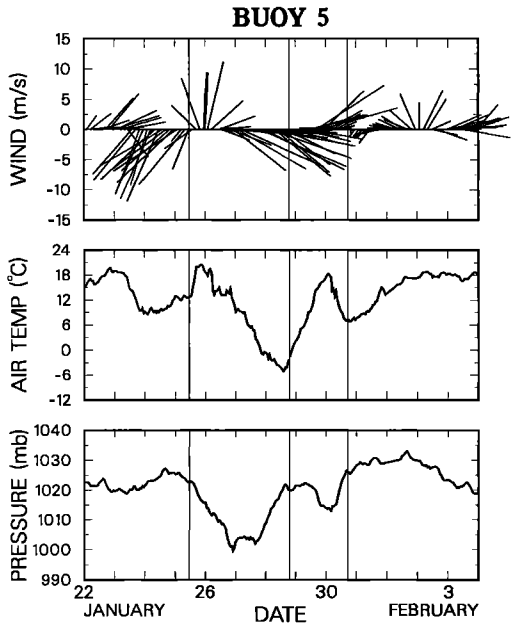

Fig. 2. Near-surface wind, air temperature and atmospheric pressure measured over the outer continental shelf by GALE buoy 5 during late January and early February 1986. (The location of buoy 5 is shown in Figure 3.) Wind sticks are oriented in the direction the wind was blowing, and true north is straight up in the plot. The three vertical lines in the diagram indicate the central time of each of the three flights discussed. The effect of the coastal front may be seen at about the time of the first flight, with winds changing from northeasterly to southeasterly as the air temperature abruptly rose. The stronger cold air outbreak occurred on January 27–28, and was characterized by westerly winds and low air temperatures. The second cold air outbreak occurred on January 30 and had northerly winds and cold temperatures, although not as cold as those on January 28.

GOES images are from January 25, 28, and 30, the days on which we conducted the P-3 and Electra flights to be described below. GALE buoy 5 was located on the outer continental shelf in the vicinity of the flight tracks. Figure 3 shows the locations of the flight tracks on the three days and the locations of GALE buoys 5 and 6. A schematic representation of the salient oceanographic features in the study area is included in this diagram. The temperature front found along each side of the Gulf Stream and the mid-shelf temperature front played important roles in determining the spatial structure of the air-sea interaction processes, as will be shown below. The mid-shelf front is a boundary between very cool inner shelf waters and warmer outer shelf waters, which are formed from a mixture of shelf and Gulf Stream waters [*Oey*, 1986]. The shoreward Gulf Stream front can be spatially complex because of meanders and frontal eddies which often progress along the stream's edge [*Bane et al.*, 1981; *Lee et al.*, 1981, this issue]. A frontal eddy with a surface warm filament is indicated schematically in Figure 3.

A low-pressure center (L) was positioned over the northern Great Lakes on January 25, and a mass of very cold, continental air was poised to its northwest behind a strong cold front (Figure 1*a*). (This is the cold air that moved down across the United States during the next few days and comprised the cold air outbreak of January 27–28 in the GALE region.) A weaker cold front stretched from the low-pressure center eastward and then southward across the central United States. A minor frontal wave was present on that front near the Louisiana-Mississippi gulf coast. Offshore on January 25 a coastal front (dashed line) had formed in the vicinity of the shoreward Gulf Stream front and was moving slowly landward [*Bosart*, 1988; *Riordan and Wang*, 1988]. The buoy data in Figure 2 show that the winds shifted from northeasterly to southeasterly and the temperature rose abruptly as the coastal front passed the buoy location on January 25. Aircraft data shown below reveal several other properties of this front. (Southeasterly to southwesterly warm air flow over the ocean is referred to herein as "pre-storm" conditions.)

On January 28 the primary low-pressure center (L) was located north of Maine. Associated with its cyclonic circulation, the strong cold front and the cold air behind it had moved across the central and eastern United States and out over the ocean (Figure 1*b*). The air flow over the shelf and Gulf Stream in the study area

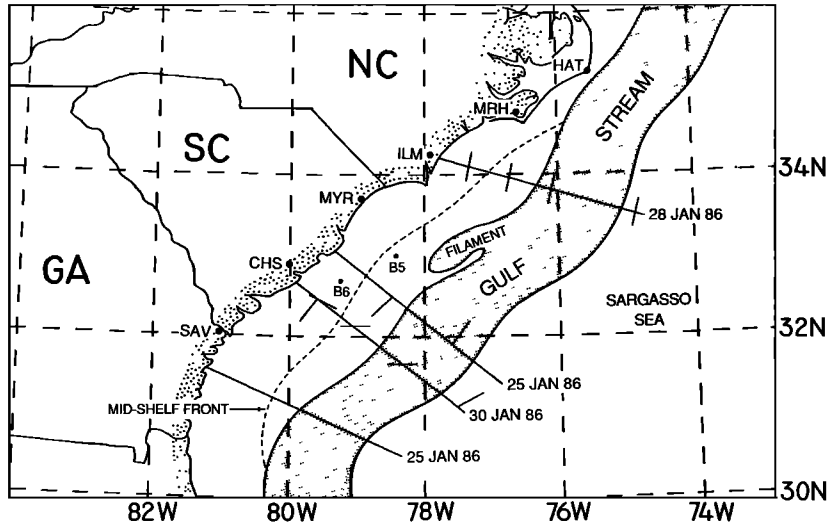

Fig. 3. A map of the study area showing the the flight tracks flown on January 25, 28, and 30. The short lines crossing the flight tracks (on all but the southern track of January 25) show the locations of the stacks flown for turbulence measurements. Important oceanographic features of the area are indicated schematically. The Gulf Stream with a warm filament along its shoreward edge is shown, as is a typical mid-shelf front separating cool inner shelf waters from warmer outer shelf waters. The Sargasso Sea is the open ocean region seaward of the Gulf Stream in this part of the North Atlantic.

was westerly to northwesterly at speeds near 15 m s^{-1}, and the air temperature had fallen to its lowest value of the period. Buoy data in Figure 2 show that air temperatures near -5°C existed over the outer shelf on January 28. This cold air outbreak provided some of the strongest thermal forcing of the ocean during GALE.

Another cold front moved through the area early on January 30 as a result of a secondary low-pressure center (L_2, Figure 1*c*), which had formed over the central United States 2 days earlier and had then moved eastward. Air temperatures fell again and northerly wind speeds increased over the Gulf Stream. Aircraft data presented below show that northerly wind speeds over the Gulf Stream were about 9 m s^{-1}, but the data in Figure 2 show that surface winds were less than 5 m s^{-1} at buoy 5 on the outer shelf. Although air temperatures were not as low during this cold air event as on January 28, the thermal forcing of the Gulf Stream was still quite strong, as will be shown below.

ATMOSPHERIC AND OCEANIC STRUCTURE

The non-turbulent structure of the MABL and the upper ocean thermal structure on January 25, 28, and 30, 1986, are discussed in this section. The locations of the vertical sections flown on those dates are shown together in Figure 3. Two sections were flown on January 25 and one was flown on each of the other days. No atmospheric turbulence measurements were made on the southern section on January 25; only the northern section from that day will be discussed here. The study was planned to provide repeated sections along a flight track off Charleston, South Carolina (CHS in Figure 3) that was nearly coincident with the ship track over the shelf there [*Atkinson et al.*, this issue]. The P-3, however, experienced a mechanical problem on January 28, which prevented it from flying that day, and airspace restrictions offshore of Charleston did not permit the P-3 sections flown in that area on January 25 and 30 to be coincident. Significant meteorological differences did not exist in the along–Gulf Stream direction over the separation distances of these sections, though. We focus here on the MABL changes in the cross-Gulf Stream direction on each day.

The vertical sections presented in this section show the thermal structure within the upper 350 m of the ocean (excluding January 28 sections, since the Electra did not make AXBT measurements) and the structure of wind speed, wind direction, air temperature and relative humidity in the lower 1500 m or so of the atmosphere. SST profiles from PRT-5 (a Barnes Precision Radiation Thermometer) measurements along the flight tracks are shown at the bottom of each section for every flight day. Atmospheric data on these sections were collected with the slow rate sensors on board each aircraft.

January 25 Sections

Recall that the January 25 sections were made during pre-storm conditions, with warm, moist air flowing from the ocean northwestward across the Gulf Stream and outer shelf. Sections showing atmospheric and oceanic structure off Charleston on this date are shown in Figure 4. The MABL had little lateral variation and a relatively constant thickness of about 1000 m over the Gulf Stream, implying only slight lateral variation in the modification of the marine air due to air-sea interaction as it flowed northwestward across the Gulf Stream. Notice in Figure 4*c* the warmest air was over the Gulf Stream core (~210 km along the section) and a Gulf Stream filament (~100 km along the section), where temperatures were only about 2°C above those on either side of the Gulf Stream. Relatively large variations in all measured atmospheric variables occurred over the outer shelf; however, these were due to the coastal front that was moving shoreward through that area at this time.

The Gulf Stream was defined well by its SST profile and subsurface structure. Its near-surface core had temperatures above 24.7°C, and a clear SST front was seen on both the shoreward side (~160 km from shore) and the Sargasso Sea side (~265 km from shore) of the stream. Interestingly, the seaward front had a greater SST gradient than the shoreward front at this time. There was a warm filament of Gulf Stream water located over the upper continental slope, and mild isotherm doming was observed between the slope and the main body of the stream.

January 28 Sections

Figure 5 shows the vertical sections of atmospheric structure as measured by the Electra on January 28. These data were collected during the stronger cold air outbreak of January 27 and 28 (compare with Figure 2). Recall that no AXBTs were deployed from the Electra, so no subsurface ocean thermal structure is shown. The SST profile measured along the section by the Electra's PRT-5 is shown at the bottom of each section. The Gulf Stream's shoreward (seaward) SST front may be seen at about 115 km (250 km) along the section.

Low level winds were westerly, from about 270°–290° at speeds of 9–11 m s^{-1} (Figures 5*a* and 5*b*). The air was flowing almost directly from the coast out across the shelf and Gulf Stream. The air temperature and relative humidity sections reflect the air mass modification that was occurring as a result of the ocean-to-atmosphere fluxes of heat and moisture. The air temperature increased from about -4°C to over 1°C between the shelf water region and the Sargasso Sea end of the section, while the relative humidity increased from less than 50% to over 70%. The MABL thickness increased from approximately 800–850 m over the coast to about 2300 m over the seaward edge of the stream. (More detailed accounts of the MABL structure and dynamics on this day may be found in the work of *Grossman* [1987], *Palm et al.* [1988], and *Wayland and SethuRaman* [1989].)

January 30 Sections

A northerly wind flow with speeds of about 8–9 m s^{-1} prevailed over the shelf and Gulf Stream section on January 30 (Figure 6). Although this wind was not oriented directly across the coast and shelf, the air was flowing from the land out across the cooler shelf waters and over the stream. The resulting air mass modification is indicated nicely by the temperature and relative humidity sections (Figures 6*c* and 6*d*). The near-surface air temperature increased from about 4°C near the coast to over 12°C at the Sargasso Sea end of the section, while relative humidity remained near 70–80% throughout this range. The MABL thickness increased from about 600–800 m near the coastline to 1200 m or so on the Sargasso Sea end of the section in concert with this air mass modification.

Near-surface temperatures within the Gulf Stream core (~175 km along the section) were near 23°C, about a degree lower than those observed on January 25. (A more detailed look at this change will be given below.) The subsurface doming of the isotherms at about 150–300 m over the upper continental slope is associated with the seaward deflection of the Gulf Stream and a weak warm filament along the stream's inner edge (see Figure 10 below).

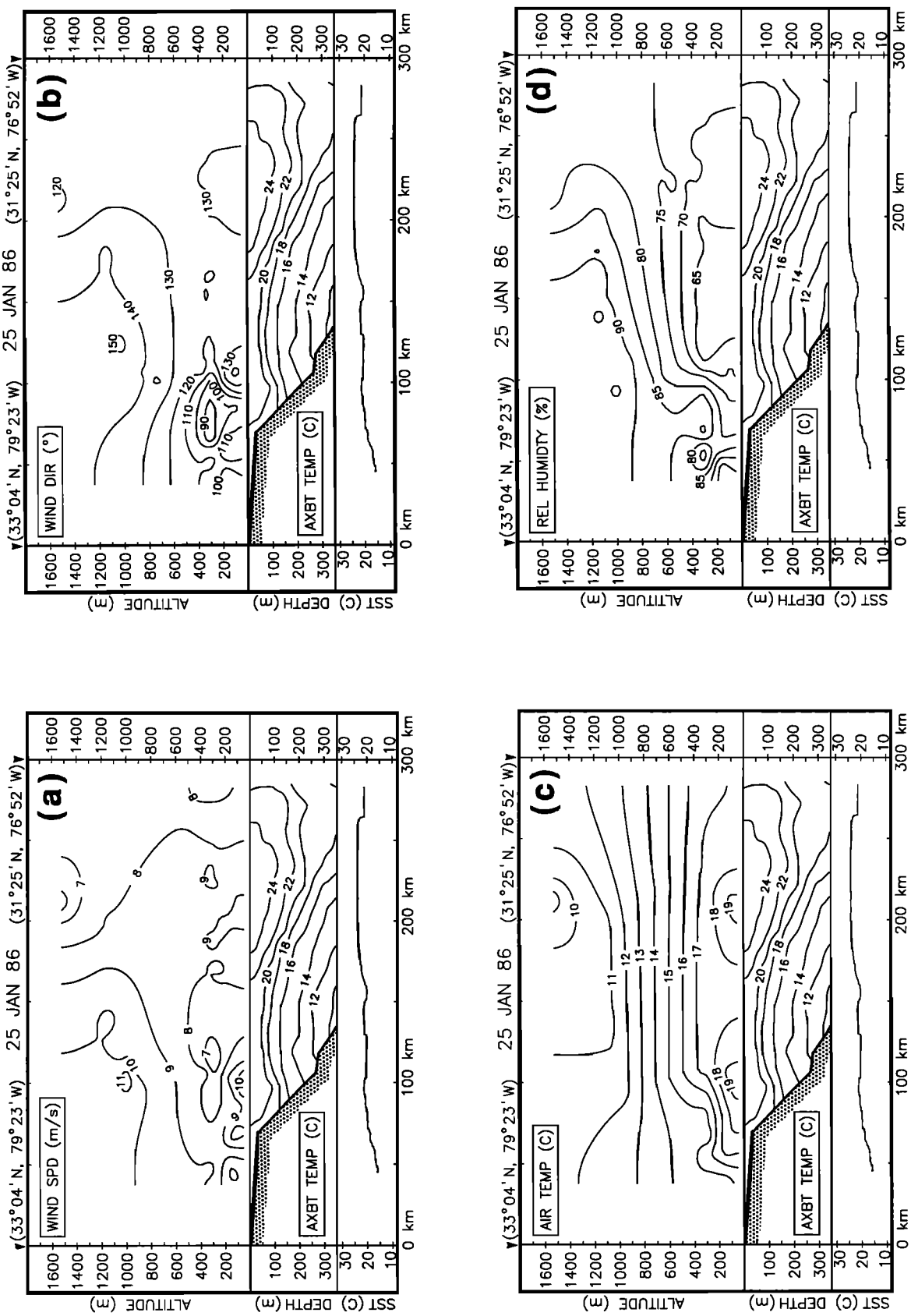

Fig. 4. Vertical sections showing atmospheric and oceanic structure along the northern flight line of January 25. Each panel shows the thermal structure in the upper 350 m of the ocean and the atmospheric structure in its lower 1500 m or so. The sea surface temperature profile measured by the aircraft's radiometer is shown at the bottom of each panel. The four panels show (*a*) wind speed, (*b*) wind direction, (*c*) air temperature, and (*d*) relative humidity. The wind flow was generally from the southeast, although the structure of the coastal front, which may be seen over the shelf portion about 50–100 km from shore, caused variations in wind direction.

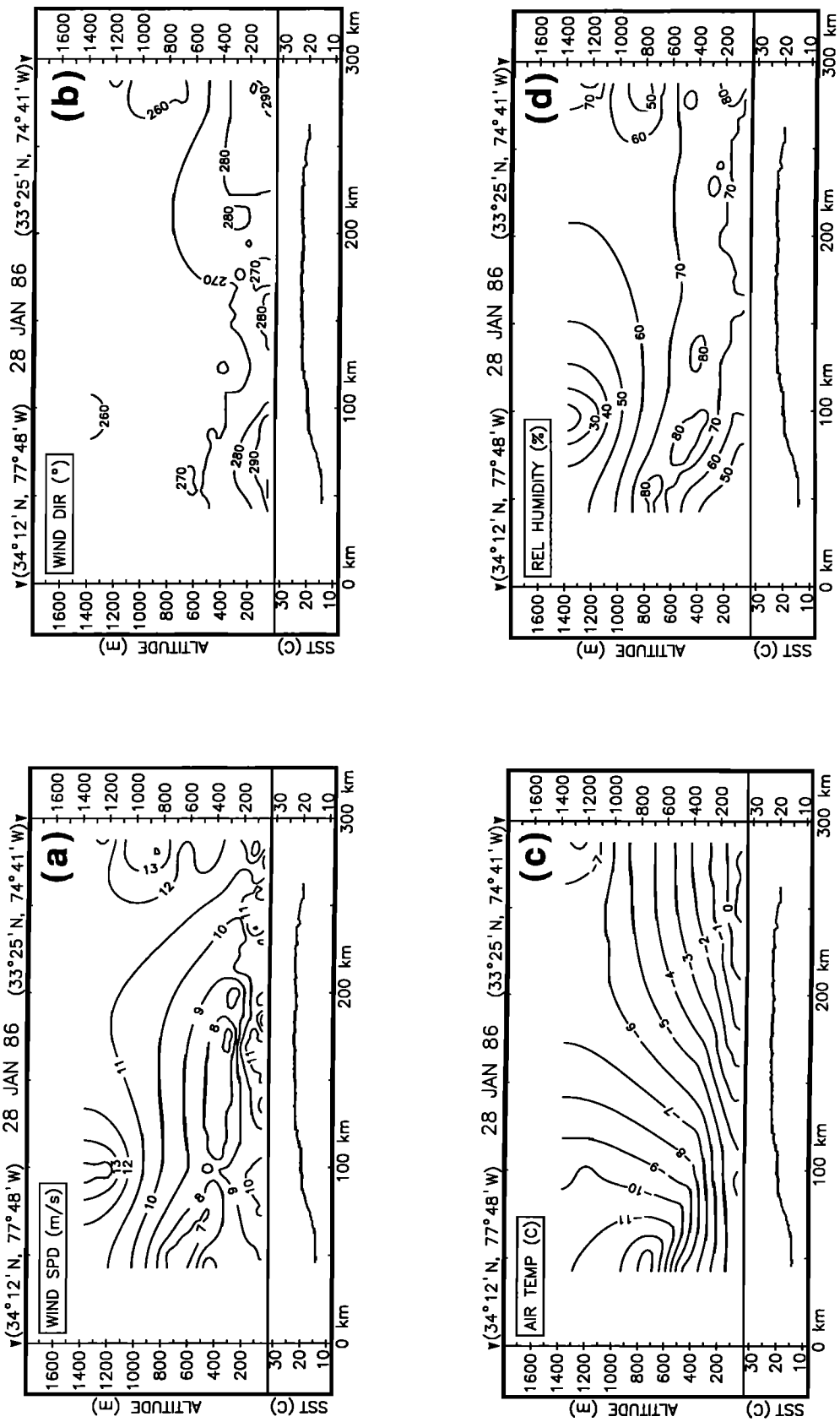

Fig. 5. As in Figure 4 but for January 28 without the subsurface ocean thermal structure (no AXBTs were deployed from the Electra). Strong westerly winds during this cold air outbreak resulted in heating and moistening of the MABL air, as indicated in Figures 5*c* and 5*d*.

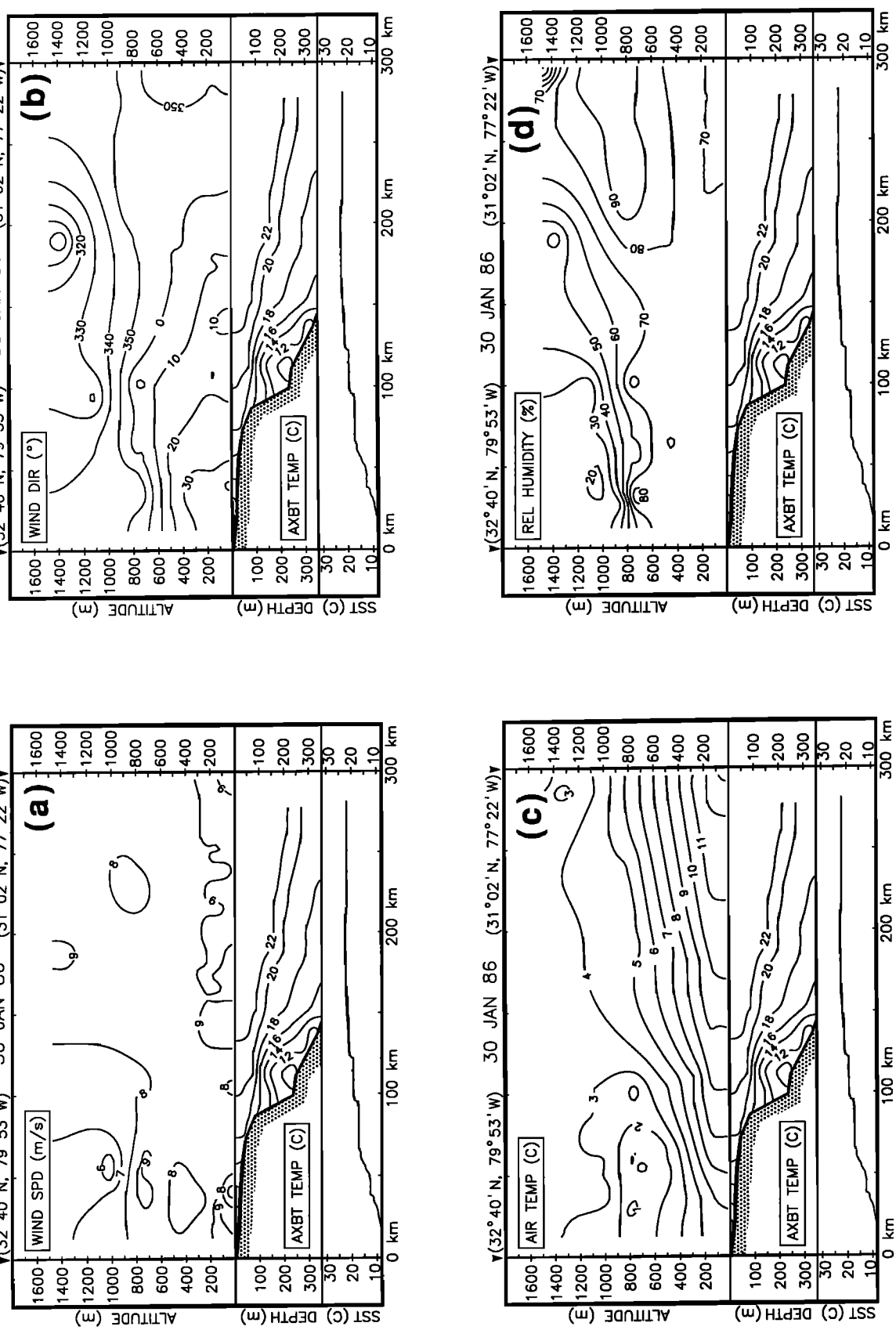

Fig. 6. As in Figure 4 but for January 30. The cold, northerly air flow on this date induced air mass modification in the MABL over the ocean, as indicated in Figures 6*c* and 6*d*.

TURBULENT FLUXES

Vertical, turbulent fluxes of momentum, heat and moisture were determined for the three flights at various locations and levels within the MABL. Profiles of these fluxes are shown in Figures 7 and 8, along with the oceanic thermal structure in a manner similar to the previous vertical sections. Under most circumstances the aircraft were able to fly at altitudes as low as 50 m over the ocean surface. The fluxes discussed here as "near-surface" fluxes are those computed from data taken on the stack leg at the lowest altitude flown for that stack. No extrapolation down to the sea surface has been attempted. The momentum fluxes are displayed in Figure 7 in a fashion which gives the correct sign for stress exerted on the surface directly below the stack level. The heat fluxes displayed in Figure 8 are the fluxes upward from below.

Momentum Fluxes

Momentum fluxes on January 25 were modest near the sea surface (less than 0.15 N m^{-2}) at both the outer shelf location and the Gulf Stream location. The vertical structure was different at the two locations, however. Total momentum flux decreased with height up to 1000 m over the outer shelf, while an increase in flux was observed upward to about 700 m followed by a decrease upward to 1500 m over the Gulf Stream. This spatial difference in the vertical structure is a result of the landward moving coastal front on that date. The leading edge of the warm, maritime air was at the location of the outer shelf stack at the time of these measurements (see Figure 4). Thus the seaward stack was entirely within the warm air, while the shoreward stack was within the frontal zone itself.

Near-surface momentum fluxes on January 28 were the strongest observed on any of the three flights. The total flux was 0.65 N m^{-2} over the shoreward edge of the Gulf Stream and ranged between 0.21 and 0.36 N m^{-2} on the other stacks. Directional variations were seen, but the stress on the ocean surface (assuming it was in the same direction as the lowest level momentum flux at each stack) was generally toward the east; the exception was over the core of the Gulf Stream where it was southward. Note that cloud cover over the stream prevented any stack legs from being flown there at altitudes over about 200 m.

During the strong southward winds on January 30 the near-surface momentum fluxes were greatest over the Gulf Stream, with a total magnitude of over 0.2 N m^{-2}. Over the shelf waters the momentum fluxes were dramatically lower, with a total magnitude of only about 0.03 N m^{-2}. In each of the four profiles there appears a mid-level maximum in flux magnitude.

Heat Fluxes

With the exception of the outer shelf sensible heat flux profile, all profiles on January 25 have a clear mid-level maximum (Figure 8*a*). This is believed to be a result of the movement of the coastal front through the region on January 25. Recall that the warm, maritime air was just passing the location of the outer shelf profile at this time (see Figure 4). Near-surface fluxes of sensible heat were very low at both profile locations, while the latent heat fluxes were about 200 W m^{-2} at the outer shelf location and near 260 W m^{-2} over the Gulf Stream.

The strong flow of cold, dry air out over the ocean during the cold air outbreak of January 28 produced the highest heat flux values measured by the aircraft during this study period (Figure 8*b*). Flux profiles decreased with height for all but the Sargasso Sea stack (about 260 km along the section), typical of cold air outbreak situations [*Grossman*, 1987; *Wayland and SethuRaman*, 1989]. Near-surface fluxes increased with distance from shore to the Gulf Stream core but then decreased somewhat as the air reached the slightly cooler Sargasso Sea waters. Near-surface sensible (latent) heat flux was about 200 (350) W m^{-2} over the inner shelf, while over the Gulf Stream core it had increased to 320 (710) W m^{-2}. (The data shown in Figure 8*b* were kindly supplied by R. Wayland and S. SethuRaman.)

Heat flux profiles on January 30 all exhibit decreasing values with height, again due to the cold, dry air flow over the warm shelf and Gulf Stream waters (Figure 8*c*). (The sensible heat flux value at the 750–m level over the inner shelf is believed to be in error.) Maximum near-surface fluxes were observed over the core of the stream, where sensible heat flux was almost 200 W m^{-2} and latent heat flux was just over 500 W m^{-2}. Near-surface fluxes at the outer shelf and Sargasso Sea locations were slightly lower than these values, while those over the inner shelf were quite low. Latent plus sensible heat fluxes over the inner shelf totalled little more than 100 W m^{-2}.

Comparison Between Aircraft-Determined and Buoy-Determined Heat Fluxes

Blanton et al. [this issue] have computed time series of sensible and latent heat fluxes from the Buoy 5 and Buoy 6 data with the use of bulk aerodynamic formulae developed by *Liu et al.* [1979]. Here we compare those fluxes with the fluxes computed from aircraft data gathered on the stacks flown over the shelf waters. For each P-3 flight near-surface data from a stack flown close to a buoy are compared with that buoy's data. For the Electra flight data taken on the second stack from shore are compared with data from Buoy 5. Although these two locations are separated by some distance alongshore, they were each within the domain of the outer shelf waters. This comparison must be viewed with some degree of caution, since the aircraft stacks were not flown precisely over the buoy locations (see Figure 3) and the aircraft stack altitudes were typically several tens of meters above the ocean surface.

The fluxes to be compared are shown in Table 1. With the exception of the latent heat flux on January 25, the buoy-determined fluxes are all greater than the aircraft-determined fluxes by amounts ranging from 12% (January 28 latent heat flux) to more than 200% (January 25 and January 30 sensible heat fluxes). A simple extrapolation of each of the flux profiles shown in Figure 8 down to buoy sensor level (3 m) does not alter these differences significantly. Rapid temporal changes occurred at the buoys on both January 25 and 30 [*Blanton et al.*, this issue], and they introduce variations that may contribute to the differences. Recall that the coastal front was progressing shoreward across the shelf on January 25, and it is likely that it had an important impact on the flux fields then. No meteorological buoys were deployed in the Gulf Stream, so no similar comparison may be made for the Gulf Stream region.

We may also consider the method of *Liu et al.* [1979] using aircraft data alone. This method states that the ocean-to-atmosphere flux of sensible heat is proportional to the air-sea temperature difference times wind speed and that the latent heat flux is proportional to the specific humidity just above the sea surface minus that at the sea surface (where the air is assumed to be at 100% relative humidity) times the wind speed. This implies that the spatial and temporal variations in the upper ocean thermal field and the MABL wind, thermal, and moisture fields that existed on the 3 days studied here would contribute to the

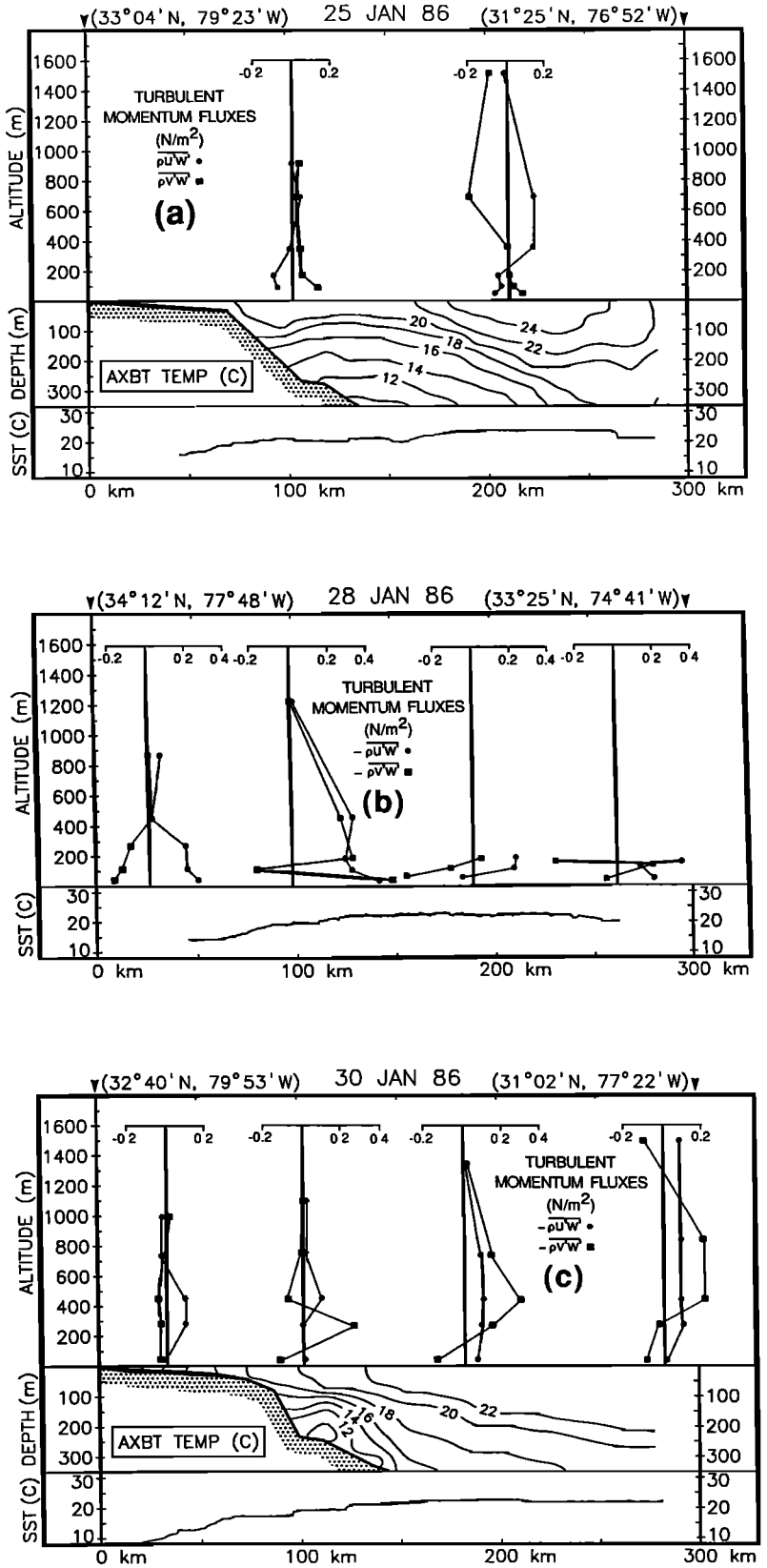

Fig. 7. Vertical, turbulent momentum fluxes within the MABL for (*a*) January 25, (*b*) January 28, and (*c*) January 30. The presentation formats are similar to those used in Figures 4–6. Modest near-surface momentum fluxes occurred during the pre-storm conditions of January 25, with magnitudes less than 0.2 N m^{-2}(Figure 7*a*). The strong westerly winds on January 28 resulted in near-surface fluxes greater than 0.4 N m^{-2} along the shoreward Gulf Stream front (Figure 7*b*). During the second, weaker cold air outbreak of January 30 near-surface momentum fluxes were about 0.2 N m^{-2}, except over the shelf where they were very low (Figure 7*c*). (Data from January 28 supplied by R. Wayland and S. SethuRaman.)

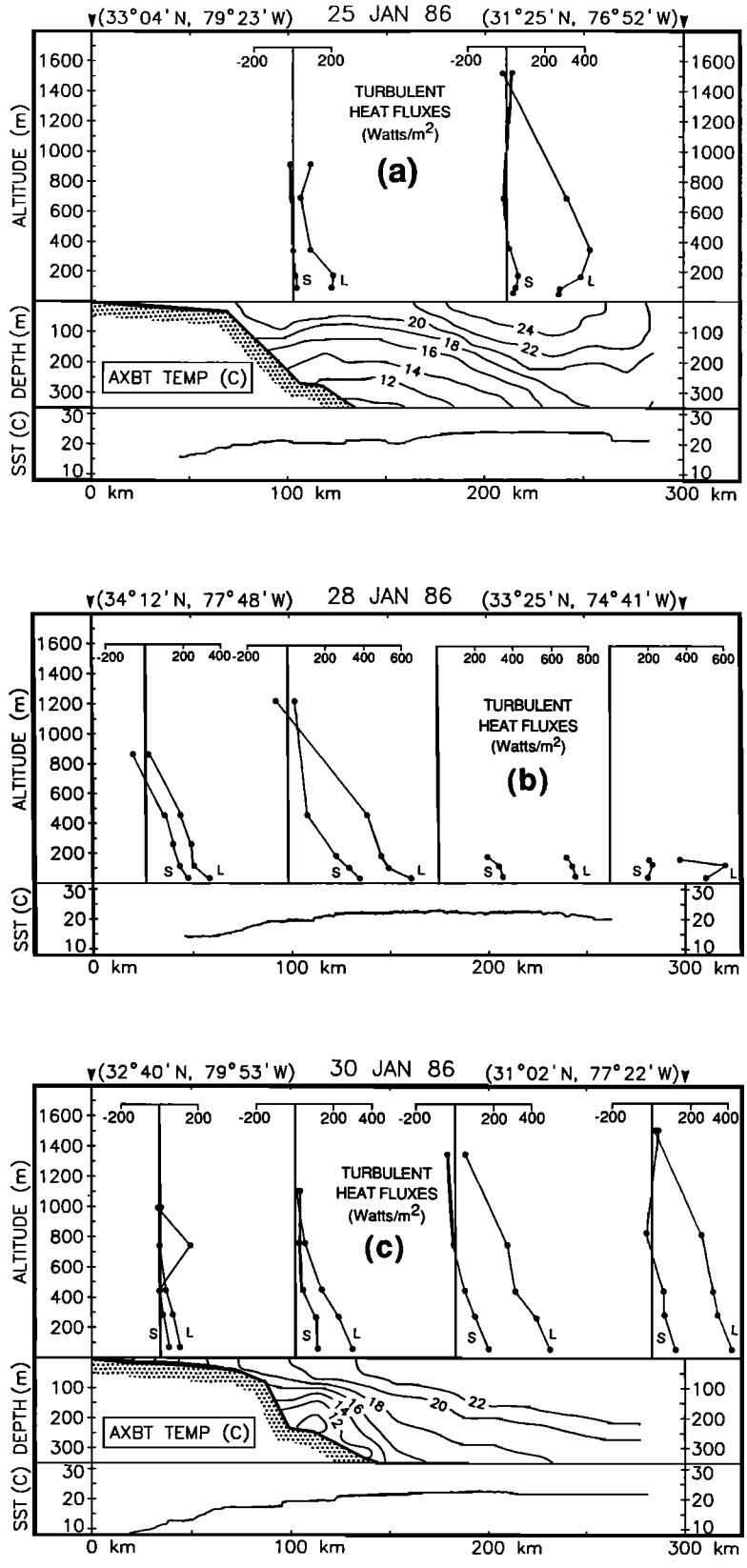

Fig. 8. Vertical, turbulent fluxes of sensible (S) and latent (L) heat within the MABL for (*a*) January 25, (*b*) January 28, and (*c*) January 30. The presentation formats are similar to those used in Figures 4–7. Total heat fluxes depended on both atmospheric conditions and ocean region, with lower heat fluxes ocurring over the inner shelf waters and during pre-storm contitions, while higher heat fluxes were found over the Gulf Stream and during cold air outbreak conditions. (Data from January 28 supplied by R. Wayland and S. SethuRaman.)

TABLE 1. Comparisons of Sensible and Latent Heat Fluxes Calculated With Aircraft- and Buoy-Measured Data

Date	Flux Type	Calculated Heat Flux, W m^{-2}			
		Buoy 5	Buoy 6	Nearest Aircraft Stack	Altitude of Stack
Jan 25	sensible	25		7	90 m
	latent	125		186	
Jan 28	sensible	500		362	32 m
	latent	700		626	
Jan 30	sensible		110	35	48 m
	latent		215	86	

structure observed in the near-surface flux field. Using aircraft data from the lowest altitude leg in each stack, the sensible (latent) heat fluxes are compared with the air-sea temperature difference times wind speed (specific humidity difference times wind speed). This comparison, shown in Figure 9, indicates that the aircraft data collected on the three GALE flights discussed here and the turbulent fluxes computed therefrom are consistent with a relationship of the form suggested by *Liu et al.* [1979]. An exchange coefficient was determined in each case with a linear regression that was forced through the origin. The values found for the exchange coefficients C_H and C_E are 0.9 x 10^{-3} and 1.3 x 10^{-3}, respectively. These are close to the values reported by *Liu et al.* [1979], which were both about 1.3–1.4 x 10^{-3} for comparable atmospheric conditions (i.e., wind speed, air-sea temperature difference, and relative humidity).

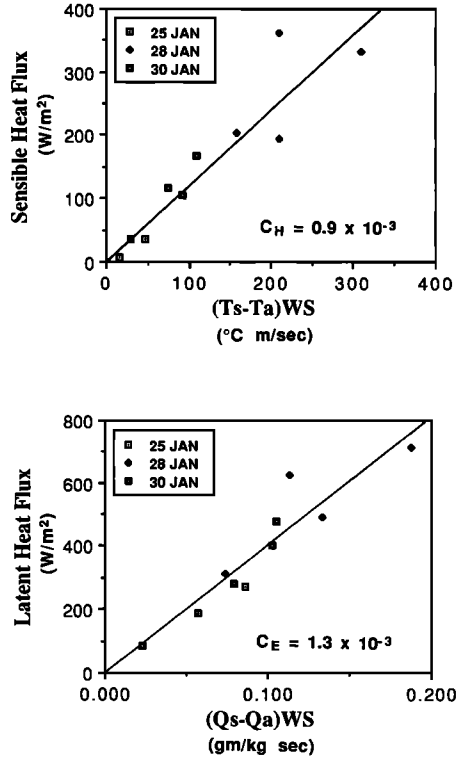

Fig. 9. (top) Near-surface sensible heat fluxes versus air-sea temperature difference multiplied by wind speed, and (bottom) near-surface latent heat fluxes versus near-surface/surface specific humidity difference multiplied by wind speed. This comparison shows how consistent the aircraft-measured near-surface fluxes are with the bulk parameterization formulae discussed by *Liu et al.* [1979]. The exchange coefficient for each heat flux is shown, and they compare well with the values of about 1.3–1.4 x 10^{-3} determined by Liu et al.

GULF STREAM THERMAL RESPONSE

Gulf Stream Path Considerations

Ocean temperatures measured with AXBTs reveal the changes that occurred in the oceanic mixed layer along the Charleston line between January 25 and 30. Recall that these two sections were not coincident in space, with the section from January 30 having been flown about 65 km to the southwest of the January 25 section. We will consider the mixed layer changes in similar regions of the sections that were caused by the atmospheric forcing during the intervening period, and we will assume that the differences in section locations alongshore have a small effect when compared to these.

Two satellite SST images are shown in Figure 10 and in Plate 1. (Plate 1 can be found in the separate color section in this issue.) These are the cloud-free images which are closest in time to the flights on January 25 and 30. A flight track is shown on each, as are the GALE current meters with daily current vectors. Cloud cover prohibited the availability of a satisfactory image on January 28. The flight of January 25, the track of which is depicted on the January 22 image, extended from the nearshore region to the Sargasso Sea side of the Gulf Stream. The flight track crossed a warm Gulf Stream filament located just seaward of the shelf break on January 25, and it was over this filament that the northwestern stack was flown (see Figures 7*a* and 8*a*). Two filaments may be seen in the January 22 image near the flight line. One was trailing the meander crest that was located southwest of the shoreward stack position at that time, and one was due south of the stack position (Figure 10, Plate 1). It is likely that the former of these two features propagated "downstream" in the intervening 3 days to be under the shoreward stack on January 25; however, clouds prevented satellite viewing of the sea surface during that 3-day period, so ambiguity does exist in this matter. Note that the currents measured at the edge of the shelf were significantly affected by the Gulf Stream and its filaments (see *Lee et al.* [this issue] for a complete discussion of the current meter measurements). The southeastern stack on January 25 was flown over the core of the Gulf Stream (Figures 7*a*, 8*a*, and 10 and Plate 1). Notice the slight seaward deflection of the body of the Gulf Stream just to the southwest of the flight line. This is the well-documented seaward deflection of the Gulf Stream offshore of Charleston [*Brooks and Bane*, 1978; *Pietrafesa et al.*, 1978; *Legeckis*, 1979; *Bane and Dewar*, 1988].

The flight on January 30 covered a cross-shelf and cross-stream distance comparable to the flight on January 25, extending from the shoreline to the offshore side of the Gulf Stream; however, four stacks were made on this flight as opposed to two (bottom panels, Figure 10 and Plate 1). They were positioned over the various oceanic temperature regimes, beginning with the cool inner shelf water near the coast. The second stack offshore was

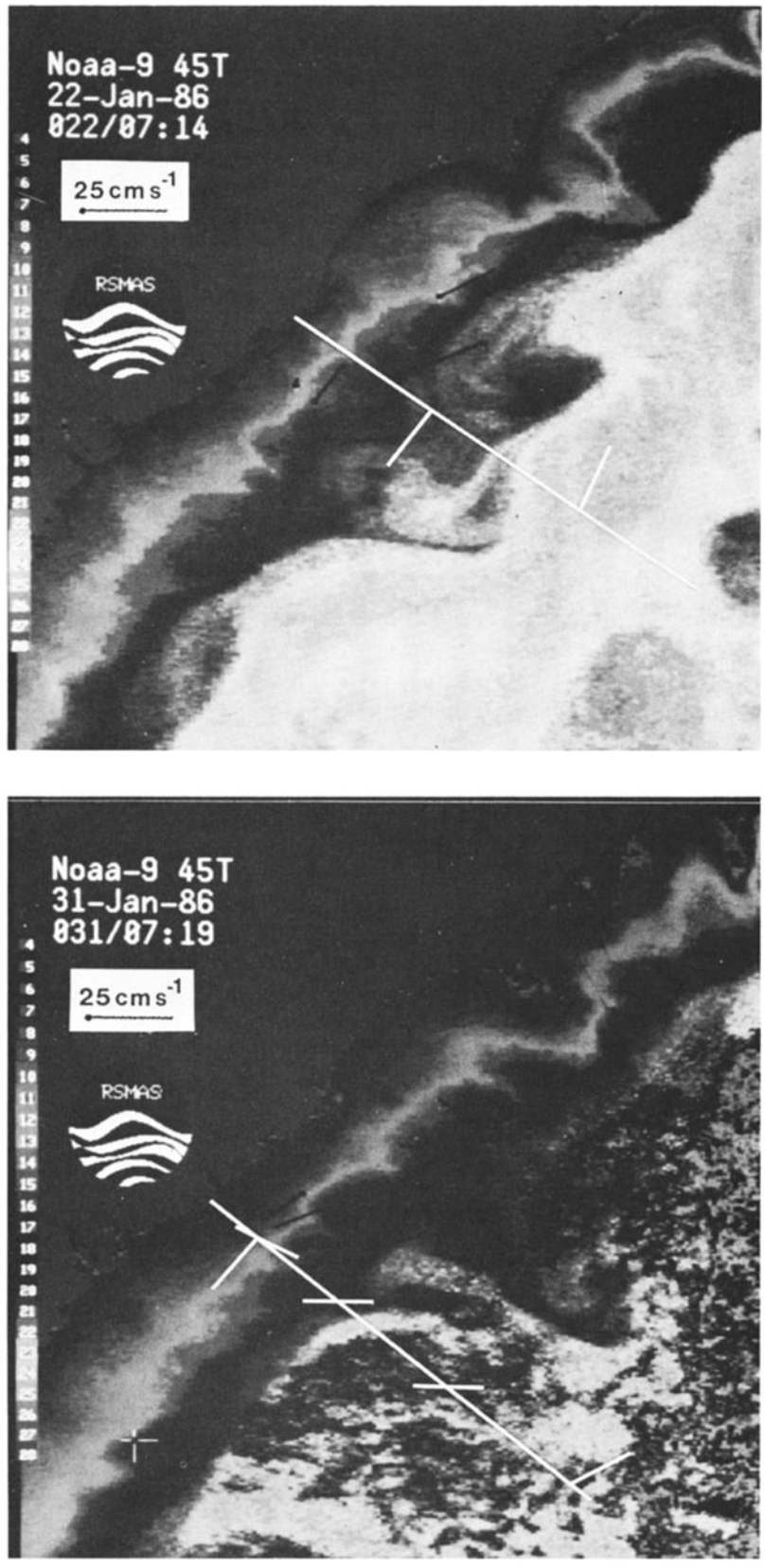

Fig. 10. Satellite sea surface temperature images showing the flight tracks over the shelf and Gulf Stream waters. (See also Plate 1.) Flight tracks (longer white lines) and stack pattern legs (shorter white lines) are indicated, and the GALE current meters are shown with daily currents in black. The flight track of January 25 is shown in the January 22 image (top), and the January 30 flight track is shown in the January 31 image (bottom). Cloud cover prevented recovery of a satisfactory image on days closer in time to these flights. Ocean surface temperatures range from below 10°C near the coast to about 26°C in the core of the Gulf Stream. The positions of the flight tracks and locations of the stacks relative to the ocean temperature regimes may be seen clearly here. (Images prepared by O. Brown and R. Evans.)

over the warmer outer shelf water, the third one was over the core of the Gulf Stream, and the last one was along the Sargasso Sea side of the stream. Note how the seaward deflection of the stream had amplified between the two images in Figure 10. (*Lee et al.* [this issue] discuss the changes in the shelf currents associated with this strengthening in the deflection.)

Mixed Layer Structure and Evolution

The vertical ocean temperature sections from the two flights are shown in Figure 11. The mixed layer, shaded in each panel, is seen to generally deepen in a seaward direction on each day. On January 25 it was about 20–40 m deep over the outer shelf and deepened to about 100–150 m near the seaward end of the section, along the Sargasso Sea side of the Gulf Stream. An area of locally deep mixed layer may be seen about 110 km from shore, which was within the Gulf Stream filament that was located there (see Figure 10). The seaward deepening of the mixed layer base within the stream followed approximately the 24°C isothermal surface until it reached the offshore end of the section. There was a double mixed layer observed near the core of the Gulf Stream, and the upper mixed layer portion there is indicated by the cross-hatched area. Mixed layer depths along the section measured on January 30 were consistently deeper, and near-surface temperatures were lower than those on January 25. The shelf portion observed on January 30 was essentially mixed throughout the water column, and the mixed layer depth increased seaward from the shelf break to about 200 m along the seaward edge of the stream. Again there was a double mixed layer region within the core of the Gulf Stream. It is indicated by the vertically hatched area.

Quantitative comparisons of mixed layer depth, temperature, and heat content were made for the Gulf Stream portions of the two sections. This was done after shifting the data along the sections in order to align them at the position of the shoreward Gulf Stream surface front. This was necessary because the stream's path had evolved somewhat between the two flights and

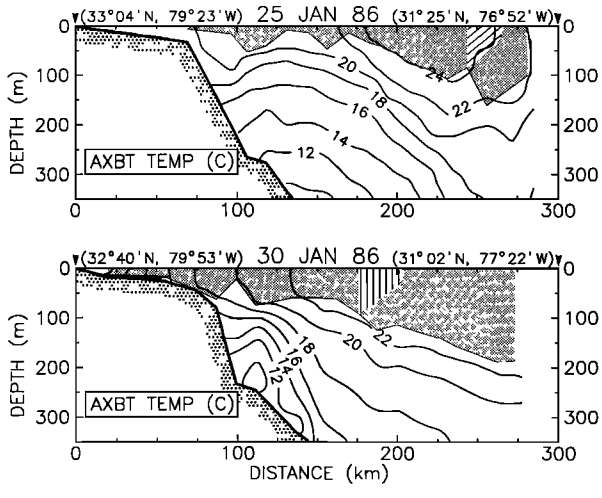

Fig. 11. Cross-stream ocean temperature sections for the (top) January 25 and (bottom) January 30 flights. The mixed layer is shaded in each section, and the upper mixed layer in the region of double mixed layer is indicated on each day with a cross-hatching (25) or vertical hatching (30). The mixed layer base was seen to slope downward in the seaward direction on each day, and there was mixed layer deepening of about 35 m (cross-sectional average) between the 2 days.

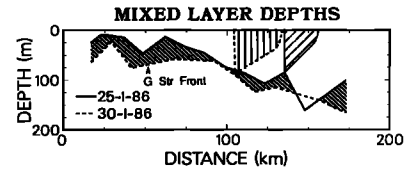

Fig. 12. Mixed layer depth profiles from the January 25 and 30 flights. These profiles have been aligned at the shoreward Gulf Stream front. The deepening between the 2 flight days may be seen (bold cross-hatched area), and the upper mixed layer in the double mixed layer region on each day is indicated in the same fashion as in Figure 11.

because the two flight lines were offset from one another. This shifting prohibits a similar comparison for the shelf region.

The "aligned" mixed layer depth profiles (Figure 12) show the deepening which occurred between the 25th and the 30th. The areas of double mixed layer are also indicated as they were in Figure 11. Two computations of average mixed layer depth across the Gulf Stream portion of the section were done, one using all AXBTs shown in Figure 12 and one beginning with the AXBT just seaward of the front. The average amounts of deepening in the two computations were 33.5 m and 35.5 m. The actual deepening is indicated by the bolder cross-hatched area in Figure 12. (In one small area the mixed layer depth on the 25th exceeded that on the 30th.)

A closer look at the double mixed layer region is given in Figure 13, which shows the actual AXBT profiles taken in those areas. Profiles from both days show that the warmer, single mixed layer to the left of the double mixed layer region shallows seaward and becomes the upper portion of the double mixed layer, while the cooler, single mixed layer to the right continues under the warmer water and becomes the lower portion of the double mixed layer. This structure is believed to be a result of the flow within the core of the Gulf Stream jet, which has brought the warmer upper mixed layer water swiftly from the south, thereby allowing it to override the cooler mixed layer water below. (Note that there are

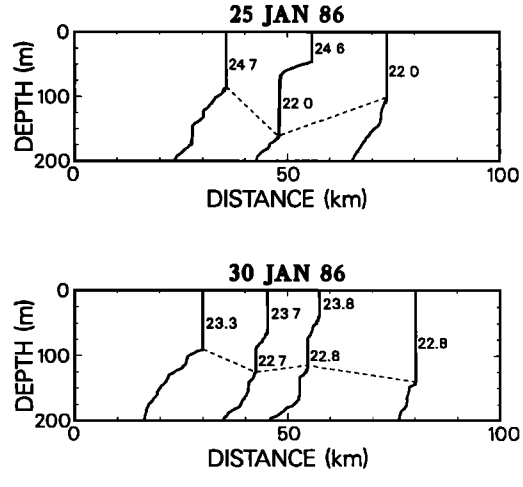

Fig. 13. A closer look at the double mixed layer structure in the Gulf Stream core. On January 25 there was only one AXBT profile recovered in the double mixed layer region, while there were two on January 30. Mixed layer temperatures are shown for each profile. On each day the warmer, single mixed layer to the left of the region shallows seaward and becomes the upper portion of the double mixed layer. The cooler, single mixed layer to the right continues under the warmer water and becomes the lower portion of the double mixed layer.

indications of other, smaller mixed layers even deeper than the mixed layer delineated by the dashed line. These may be remnants of earlier surface mixed layers or may be the result of small-scale, internal instability and mixing processes.)

Heat Content Change

Because of the northward flow of the Gulf Stream the flights on January 25 and 30 did not measure the same parcel of water. Nonetheless, relatively large changes that occur in the local, upper layer structure within a few days may be viewed as a result of excessive atmospheric forcing (excluding, of course, events such as a ring–Gulf Stream interaction). Consider the following. The average wintertime atmospheric cooling of the Gulf Stream is roughly sufficient to lower the stream's surface temperature as it flows northward while leaving the local temperature unchanged; that is, a local steady state exists. In the event of excessive atmospheric cooling along a sufficiently large stretch of the current, local cooling of the upper Gulf Stream would be observed, as the water flowing from the south would have been excessively forced in a fashion similar to the local waters. This cooling would be reflected in a lowering of the local upper layer heat content, and would likely cause the mixed layer to deepen through convective overturning and wind mixing.

Figure 14 shows the upper ocean temperatures along the flight lines of January 25 and 30. The ocean "skin" temperatures measured with the PRT-5 are shown in the top panel, and the mixed layer temperatures measured by the AXBTs are shown in the bottom panel. (Only temperatures to the right of the Gulf Stream front ["G. Str. Front" arrow] should be compared.) Both skin temperatures and mixed layer temperatures decreased during the time between the two flights on the order of 1°C. Thus both mixed layer deepening and a decrease in the upper layer Gulf Stream temperatures were observed between January 25 and 30, in line with the discussion of the previous paragraph.

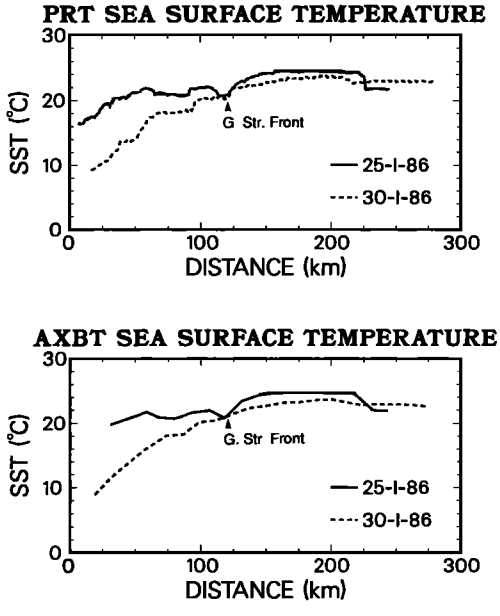

Fig. 14. Sea surface temperature profiles along the flight tracks of January 25 and 30 as determined by (top) the PRT-5 on the P-3 and (bottom) the AXBTs. These profiles are aligned at the shoreward Gulf Stream front (arrow), so shelf temperatures to the left of the front may not be compared. A temperature decrease of about 1°C is indicated, consistent with the average mixed layer heat content change of -0.62°C computed from AXBT data.

Because of the mixing which accompanies mixed layer deepening and the variations in mixed layer structure (for example, the double mixed layers in the core of the Gulf Stream), temperature changes alone may not accurately represent the effect of strong atmospheric forcing. Upper layer heat content is a better quantitative indicator of upper layer change than is temperature. Using the AXBT-measured upper layer temperatures, the heat content of a volume along the aligned sections was calculated for each flight. The volume was bounded by the ocean surface, a vertical side at the shoreward Gulf Stream front, a vertical side on the Sargasso Sea end of the section, and the base of the deeper mixed layer along the section (which is the mixed layer base on January 30 for all of the section except the short portion at about 150 km in Figure 12). The volume considered was 1 m thick in the direction normal to the section. Effects due to mixing with deeper waters are minimized by using such a volume.

The heat content change in this volume between January 25 and 30 was computed to be -3.2×10^{13} J, an amount equivalent to a volume-averaged temperature decrease of 0.62°C. For comparison, a heat flux of 500 W m^{-2} from a column of water 100 m deep acting for 5 days is sufficient to decrease the average temperature in the column 0.5°C. Recall that the near-surface latent plus sensible heat fluxes over the Gulf Stream ranged from several hundred to well over 1000 W m^{-2} on the 3 flight days; thus the computed heat content change is in line with the measured heat fluxes. Other processes not considered here, such as radiation fluxes, lateral mixing and downstream heat advection, make this simple comparison incomplete, however. A more detailed analysis of the heat budget within the Gulf Stream is beyond the scope of this paper, and will be presented in a later report.

SUMMARY

Aircraft, buoy, and satellite measurements have been used to study the wintertime air-sea interaction processes across the Gulf Stream during a 6-day period in January 1986. The turbulent flux regime in the marine atmospheric boundary layer exhibited considerable spatial and temporal variability during this 6-day period, which was related to both the evolution of the synoptic scale atmospheric conditions and the ocean surface temperature field. During the pre-storm conditions prior to January 25, the spatial structure of the SST field played an important role in generating a shallow atmospheric frontal zone along the Gulf Stream front by causing differential heating of the MABL over the stream versus over the cooler shelf waters. As this front moved shoreward on January 25, the warm, moist maritime air flowing northwestward behind the front induced moderate ocean-to-atmosphere heat fluxes (~300 W m^{-2} total heat flux measured over the core of the Gulf Stream). The subsequent outbreak of eastward flowing cold, dry, continental air over the ocean on January 27 and 28 generated high total heat fluxes (~1060 W m^{-2} measured over the core of the stream), as did a second, somewhat weaker outbreak which followed on January 30 (~680 W m^{-2} measured over the core of the stream). During each of these outbreaks, with air flowing from land out over the continental shelf, Gulf Stream, and Sargasso Sea waters, the ocean surface temperature field again affected the spatial structure of the flux fields. The near-surface fluxes of sensible and latent heat were found to be relatively low over the cool continental shelf waters, while higher fluxes were seen over the stream and Sargasso Sea. Similar spatial structure was seen in the near-surface momentum flux values, but relative changes were typically smaller from one location to another on a particular day.

The most noticeable responses of the Gulf Stream to these surface fluxes were a deepening in its mixed layer and a loss of upper layer heat; however no direct current observations were made in the stream, so velocity changes may not be assessed. An average mixed layer deepening of about 35 m was observed in the stream, and the upper layer heat loss was estimated to be 3.2 x 10^{13} J m^{-1} alongstream, an amount sufficient to decrease the average mixed layer temperature by 0.62°C. No path changes in the stream could be attributed to the atmospheric forcing of this period, since there was a large offshore movement of the stream in the region of the Charleston bump at this time due to other processes. Any path changes that may have been associated with the atmospheric forcing would have been masked by that offshore movement.

APPENDIX

On March 5, 1986, a non-IOP day, the NOAA P-3 and the NCAR Electra were flown in formation to intercompare several of the parameters measured by the two aircraft. Four straight-and-level legs of 8-min duration each were flown in an area approximately 100 km southeast of Cape Hatteras, North Carolina. The first two legs were flown at 170 m altitude and the second two at 440 m. At each altitude, two airspeeds were flown, 200 knots indicated airspeed (KIAS) (103 m s^{-1}) and 220 KIAS (113 m s^{-1}). The legs were flown crosswind, since crosswind-measured turbulent flux estimates have generally been found to be more reliable than alongwind flux estimates.

For the slow rate data (one data point per second) the quantities intercompared were pressure, radar altitude, air temperature, dew point temperature, sea surface temperature, wind direction, and wind speed. Means and standard deviations of the parameters for each leg were calculated and compared between the two aircraft. For each variable, the average mean differences between the values recorded by the two aircraft and the ranges of the mean differences are presented in Table A1.

The P-3 consistently recorded higher values for the pressure, air temperature, and dew point temperature than did the Electra for the same legs (Table A1). The Electra consistently recorded higher altitudes and sea surface temperatures. The differences in the altitudes of the aircraft would account for some, but not all, of the differences in the pressure. Therefore there seem to be consistent, real offsets between the values recorded by the P-3 and the Electra for pressure, air temperature, dew point temperature, and sea surface temperature, assuming the altitude offset to be a result of the aircraft actually being at slightly different levels. Table A1 also shows that the P-3 consistently recorded slightly greater values for the wind direction. For the wind speed, however, the P-3 recorded higher values than the Electra on legs 2 and 4 but lower values on legs 1 and 3. This suggests that there is a real, consistent offset between the wind directions recorded by the P-3 and Electra that could be taken into account; however, nothing consistent occurred for wind speed.

TABLE A1. Comparison Statistics Between the NOAA P-3 and NCAR Electra Slow Rate Data

Variable	$\langle\Delta\bar{x}\rangle$*	Range
Pressure, mbar	-1.8	-2.1 to -1.4
Altitude, m	4.0	3.0 to 7.0
Air temperature, °C	-0.3	...
Dew point temperature ,°C	-1.2	-1.3 to -1.2
Sea surface temperature, °C	1.5	1.5 to 1.6
Wind direction, deg	-4.6	-7.9 to -1.8
Wind speed, m s^{-1}	-0.4	1.4 to 0.4

Means are computed from four straight-and-level legs which were flown simultaneously.

*$\Delta\bar{x} = \bar{x}_{Electra} - \bar{x}_{P3}$.

TABLE A2. Comparisons Between the NOAA P-3 and NCAR Electra for the Vertical Fluxes of Horizontal Velocity, Humidity, and Temperature

Leg #	P-3	Electra	Difference, %
	Horizontal Velocity Flux		
1	0.29 $m^2 s^{-2}$	0.37 $m^2 s^{-2}$	-22
2	0.46 $m^2 s^{-2}$	0.45 $m^2 s^{-2}$	2
3	0.17 $m^2 s^{-2}$	0.04 $m^2 s^{-2}$*	325*
4	0.16 $m^2 s^{-2}$	0.17 $m^2 s^{-2}$	-6
	Humidity Flux		
1	0.296 g $m^{-2}s$	0.307 g $m^{-2}s$	-4
2	0.252 g $m^{-2}s$	0.288 g $m^{-2}s$	-12
3	0.176 g $m^{-2}s$	0.270 g $m^{-2}s$	-35
4	0.217 g $m^{-2}s$	0.281 g $m^{-2}s$	-23
	Temperature Flux		
1	0.198 °C m s^{-1}	0.186 °C m s^{-1}	6
2	0.181 °C m s^{-1}	0.163 °C m s^{-1}	11
3	0.097 °C m s^{-1}	0.108 °C m s^{-1}	-10
4	0.103 °C m s^{-1}	0.129 °C m s^{-1}	-20

Difference = ((P-3 - Electra)/Electra)x100

*The Electra value is suspect here.

The fast rate data (20 samples per second for the Electra and 40 samples per second for the P-3) recorded by the two aircraft were also intercompared. The quantities of interest here are the vertical fluxes of velocity ($\langle u'w'\rangle$, $\langle v'w'\rangle$), humidity ($\langle q'w'\rangle$), and temperature ($\langle T'w'\rangle$). Preliminary results of these turbulence comparisons are presented in Table A2. Here the x- and y-directed velocity fluxes have been combined into a single velocity flux. These results show that for legs 1, 2, and 4 there was good agreement between the P-3 and Electra for the vertical fluxes of velocity; however, for leg 3 there was poor agreement between the two aircraft. It seems that the leg 3 value for the Electra is suspect, since the P-3 value is consistent with the values from leg 4 while the Electra value is quite different. For the vertical flux of humidity, there was good agreement between the aircraft for all four legs. Both aircraft were also self-consistent on the reverse heading runs. For the vertical flux of temperature there was good agreement between the P-3 and Electra for all four legs. Once again, both aircraft were self-consistent on the reverse heading runs. More detailed studies of these intercomparison data are presently underway.

Acknowledgments This study benefitted from the efforts of many people associated with the GALE program. In particular, we are grateful to the expert flight crews of the NOAA P-3 and NCAR Electra aircraft who flew these missions; to the ground support personnel, especially Sam Ashwell and Al Cooper of the GALE Aircraft Operations Office and Richard Dirks, GALE Project Director; to Robert Grossman, mission scientist aboard the Electra flight of January 28; and to Richard Gilmer and Bill Otto for collecting and processing the P-3 turbulence data. We have been enlightened on the complexity of the wintertime atmosphere and ocean through discussions with Larry Atkinson, Jackson Blanton, Robert Grossman, Tom Lee, Al Riordan and SethuRaman. We are grateful to Lauren Moore Goodman for the computation of Gulf Stream heat content, and to Otis Brown, Bob Evans and Chris Velden for preparing the satellite imagery. This work was supported by National Science Foundation grant OCE-8516131 to the University of North Carolina.

REFERENCES

Adamec, D., and R. L. Elsberry, Numerical simulations of the response of intense ocean currents to atmospheric forcing, *J. Phys. Oceanogr., 15*, 273–287, 1985*a*.

Adamec, D., and R. L. Elsberry, The response of intense oceanic current systems entering regions of strong cooling, *J. Phys. Oceanogr , 15*, 1284–1295, 1985*b*.

Atkinson, L. P., E. Oka, S. Y. Wu, T. J. Berger, J. O. Blanton, and T. N. Lee, Hydrographic variability on the southeastern United States shelf and slope waters during the Genesis of Atlantic Lows Experiment: Winter 1986, *J. Geophys. Res.*, this issue.

Bane, J. M., Jr., and W. K. Dewar, Gulf Stream bimodality and variability downstream of the Charleston bump, *J. Geophys. Res., 93*(C6), 6695–6710, 1988.

Bane, J. M., Jr., D. A. Brooks, and K. R. Lorenson, Synoptic observations of the three-dimensional structure and propagation of Gulf Stream meanders along the Carolina continental margin, *J. Geophys Res., 86*(C7), 6411–6425, 1981.

Blanton, J. O., T. N. Lee, L. P. Atkinson, J. M. Bane, A. J. Riordan, and S. Raman, Oceanographic studies during project GALE, *Eos Trans AGU, 68*, 1626–1627, 1636–1637, 1987.

Blanton, J. O., J. A. Amft, D. K. Lee, and A. Riordan, Wind stress and heat fluxes observed during winter and spring 1986, *J. Geophys. Res.*, this issue.

Brooks, D. A., and J. M. Bane, Jr., Gulf Stream deflection by a bottom feature off Charleston, South Carolina, *Science, 201*, 1225–1226, 1978.

Bosart, L. F., Coastal frontogenesis and cyclogenesis during GALE IOP2, in *GALE/CASP Workshop Reports*, pp. 75-93, National Center for Atmospheric Research, Boulder, Colo., 1988.

Budyko, M. I., *Climate and Life*, 508 pp., Academic, San Diego, Calif., 1974.

Bunker, A., and L. V. Worthington, Energy exchange charts of the North Atlantic Ocean, *Bull. Am. Meteorol. Soc., 57*, 450–467, 1976.

Chou, S.-Y., and D. Atlas, Satellite estimates of ocean-air heat fluxes during cold air outbreaks, *Mon. Weather Rev., 110*, 1434–1450, 1982.

Colucci, S. J., Winter cyclone frequencies over the eastern United States and adjacent western Atlantic, *Bull. Am. Meteorol. Soc., 57*, 548–553, 1976.

Gorshkov, S. G., *World Ocean Atlas*, vol. 2, *Atlantic and Indian Oceans*, 306 pp., Pergamon, Elmsford, N. Y., 1978.

Greenhut, G. K., and R. O. Gilmer, Calibration and accuracy of the NOAA/ERL gust probe system and intercomparison with other systems, *NOAA Tech. Memo ERL ESG-22*, 30 pp., NOAA Environ. Sci. Group, Boulder, Colo., 1985.

Grossman, R. L., Boundary layer warming by condensation: Air-sea interaction during an extreme cold air outbreak from the eastern coast of the United States, in *Proceedings of the 7th Conference on Ocean-Atmosphere Interaction*, pp. 14–18, American Meteorological Society, Boston, Mass., 1987.

Gyakum, J. R., On the evolution of the QE II storm, I, Synoptic aspects, *Mon. Weather Rev., 111*, 1137–1155, 1983*a*.

Gyakum, J. R., On the evolution of the QE II storm, II, Dynamic and thermodynamic structure, *Mon Weather Rev., 111*, 1156–1173, 1983*b*.

Hayden, B. P., Secular variation in Atlantic Coast extratropical cyclones, *Mon. Weather Rev., 109*, 159–167, 1981.

Henry, W. K., and A. H. Thompson, An example of polar air modification over the Gulf of Mexico, *Mon. Weather Rev., 104*, 1324–1327, 1976.

Horton, C. W., Surface front displacement in the Gulf Stream by hurricane/tropical storm Dennis, *J. Geophys Res., 89*(C2), 2005–2012, 1984.

Horton, C. W., and L. E. Horsley, Variability in Gulf Stream surface-subsurface frontal separation: The unimportance of Ekman advection, *J. Geophys. Res., 93*(C4), 3519–3527, 1988.

Huh, O. K., L. J. Rouse, Jr., and N. D. Walker, Cold air outbreaks over the northwest Florida continental shelf: Heat flux processes and hydrographic changes, *J. Geophys Res , 89*(C1), 717–726, 1984.

Kondo, J., Heat balance of the East China Sea during the air mass transformation experiment, *J. Meteorol. Soc. Jpn., 54*, 382–398, 1976.

Lee, T. N., L. P. Atkinson, and R. Legeckis, Observations of a Gulf Stream frontal eddy on the Georgia continental shelf, April 1977, *Deep Sea Res., Part A, 28*(4), 347–378, 1981.

Lee, T. N., E. Williams, J. Wang, R. Evans, and L. Atkinson, Response of South Carolina continental shelf waters to wind and Gulf Stream forcing during winter of 1986, *J. Geophys. Res* , this issue.

Legeckis, R. V., Satellite observations of the influence of bottom topography on the seaward deflection of the Gulf Stream off Charleston, South Carolina, *J. Phys. Oceanogr., 9*, 483–497, 1979.

Liu, W. T., K. B. Katsaros, and J. A. Businger, Bulk parameterization of air-sea exchanges of heat and water vapor including the molecular constraints at the interface, *J. Atmos. Sci., 36*, 1722–1735, 1979.

Merceret, F. J., and H. W. Davis, The determination of navigational and meteorological variables measured by NOAA/RFC WP3D aircraft, *NOAA Tech. Memo. ERL RFC-7*, 21 pp., NOAA Res. Facilities Center, Miami, Fla., 1981.

Miller, E. R., and R. B. Friesen, Standard output data products from the NCAR research aviation facility, *Bull. 9*, Nat. Center for Atmos. Res., 64 pp., Boulder, Colo., 1985.

Nof, D., On the response of ocean currents to atmospheric cooling, *Tellus, Ser. A, 35*, 60–72, 1983.

Osgood, K. E., and J. M. Bane, Jr., Genesis of Atlantic lows experiment, NOAA P-3 oceanographic/boundary layer flights data report, *Tech. Rep. CMS-87-1*, Univ. of N. C., Chapel Hill, 1987.

Osgood, K. E., J. M. Bane, Jr., and R. L. Grossman, Electra-P3 intercomparison during GALE, in *GALE Preliminary Analysis Reports*, pp. 47–51, National Center for Atmospheric Research, Boulder, Colo., 1987.

Oey, L.-Y., The formation and maintenance of density fronts on the U.S. southeastern continental shelf during winter, *J. Phys. Oceanogr., 16*, 1121–1135, 1986.

Palm, S. P., S. H. Melfi and R. Boers, GALE-NASA Electra boundary layer flights data report, *NASA Tech. Memo 100703*, 1988.

Pietrafesa, L. J., L. P. Atkinson, and J. O. Blanton, Evidence for deflection of the Gulf Stream by the Charleston Rise, *Gulf Stream, 4*(9), 3–7, 1978.

Riordan, A. J., and J.-F. Wang, Mesoscale features of the early stages and onshore movement of a coastal front near Cape Hatteras, North Carolina, *GALE/CASP Workshop Reports*, pp. 95-99, National Center for Atmospheric Research, Boulder, Colo., 1988.

Sanders, F., The meteorological "bomb"; an explosive maritime cyclone, in *Proceedings of the Oceans '84 Conference*, pp. 77-89, Marine Technology Society, Washington, D.C., 1984.

Sanders, F., Explosive cyclogenesis over the west-central North Atlantic ocean, 1981–84, I, Composite structure and mean behavior, *Mon. Weather Rev., 114*, 1781–1794, 1986*a*.

Sanders, F., Explosive cyclogenesis over the west-central North Atlantic ocean, 1981–84, II, Evaluation of LFM model performance, *Mon. Weather Rev., 114*, 2207–2218, 1986*b*.

Sanders, F., and J. R. Gyakum, Synoptic-dynamic climatology of the "bomb," *Mon. Weather Rev., 108*, 1589–1606, 1980.

SethuRaman, S., A. J. Riordan, T. Holt, M. Stinder, and J. Hinman, Observations of the marine boundary layer thermal structure over the Gulf Stream during a cold air outbreak, *J Clim Appl. Meteorol., 25*, 14–21, 1986.

Stage, S. A., and J. A. Businger, A model for entrainment into a cloud-topped marine boundary layer, I, Model description and application to a cold air outbreak episode, *J. Atmos. Sci., 38*, 2213–2229, 1981*a*.

Stage, S. A., and J. A. Businger, A model for entrainment into a cloud-topped marine boundary layer, II, Discussion of model behavior and comparison with other models, *J. Atmos. Sci., 38*, 2230–2242, 1981*b*.

Wayland, R. J., and S. SethuRaman, Mean and turbulent structure of a baroclinic marine boundary layer during the 28 January 1986 cold air outbreak (GALE 86), *Boundary Layer Meteorol.*, in press, 1989.

Whittaker, L. M., and L. H. Horn, Geographical and seasonal distribution of North American cyclogenesis, 1958–1977, *Mon. Weather Rev., 109*, 2312–2322, 1981.

Worthington, L. V., *On the North Atlantic Circulation*, 110 pp., Johns Hopkins University Press, Baltimore, Md., 1976.

Worthington, L. V., Intensification of the Gulf Stream after the winter of 1976–77, *Nature, 270*, 415–417, 1977.

Zishka, K. M., and P. J. Smith, The climatology of cyclones and anticyclones over North America and surrounding ocean environs for January and July 1950–77, *Mon. Weather Rev , 108*, 387–401, 1980.

J. M. Bane, Marine Sciences Program, University of North Carolina, Chapel Hill, NC 27599.

K. E. Osgood, School of Oceanography, University of Washington, Seattle, WA 98195.

(Received June 29, 1988;
accepted August 12, 1988.)

Plate 1 [*Bane and Osgood*]. Satellite sea surface temperature images showing the flight tracks over the shelf and Gulf Stream waters. (See also Figure 10.) Flight tracks (longer white lines) and stack pattern legs (shorter white lines) are indicated, and the GALE current meters are shown with daily currents in black. The flight track of January 25 is shown in the January 22 image (top), and the January 30 flight track is shown in the January 31 image (bottom). Cloud cover prevented recovery of a satisfactory image on days closer to these flights. Ocean surface temperatures range from below 10°C near the coast (dark blue) to about 26°C in the core of the Stream (red). The positions of the flight tracks and locations of the stacks relative to the ocean temperature regimes may be seen clearly here. The SST color scale is shown on the left in each image. (Images prepared by O. Brown and R. Evans.)